WELDING RESEARCH

SUPPLEMENT TO THE *WELDING JOURNAL*, OCTOBER 2005
Sponsored by the American Welding Society and the Welding Research Council

Estimation of Cooling Rate in the Welding of Plates with Intermediate Thickness

Cooling rates estimated by Rosenthal's thick- and thin-plate solutions can be modified by a weighting factor to account for intermediate values of plate thickness

BY K. POORHAYDARI, B. M. PATCHETT, AND D. G. IVEY

ABSTRACT. An innovative method for estimating the actual cooling rate in a welded section is presented. The method is based on applying a weighting factor to the Rosenthal analytical solutions for thick and thin plates. The factor is determined from the heat-affected zone (HAZ) width, obtained from etched sections, and reflects the actual response of the plate to the heat flow condition. Previous formulations in the literature are based on the assumption of either thin-plate or thick-plate conditions, while most actual conditions lie somewhere between the two extremes. Limited experimental measurements of cooling rate, carried out by instrumented welding, showed good agreement with predicted values. The model was further used to predict the peak temperature profile across the HAZ.

Introduction

A typical arc weld thermal cycle consists of very rapid heating (several hundreds of degrees per second) to a peak temperature, followed by relatively fast cooling (a few tens or hundreds of degrees per second) to ambient temperature. The microstructural changes in the weld zone, as well as the weld heat-affected zone (HAZ), are greatly dependent on the heating and cooling rates, which in turn depend on the weld heat input (a function of arc energy, travel speed, and the thermal efficiency of the process), the plate thickness/geometry, and the initial or interpass temperature. The microstructural changes will directly affect the property changes (whether mechanical or corrosion related) in the weld zone and the HAZ. Therefore, it is important to be able to predict the actual thermal cycle characteristics such as peak temperature and cooling rate if microstructure is to be characterized and correlation with the properties is sought. This becomes more significant if the effect of heat input on the microstructural changes in the HAZ is to be examined for a given material, as the heat input is only a rough, simplified parameter specific to a welding process. Moreover, knowledge of the cooling rate is required for simulation approaches.

The most widely used and the best known analytical solutions to predict weld thermal history and cooling rate are those of Rosenthal (Refs. 1, 2). His approach was based on the assumption of a moving point heat source on the plate surface, neglecting any heat transfer from the surface. It was also assumed that physical coefficients were constant (i.e., independent of temperature), and all the energy from the welding equipment was transferred to the arc. There have been many other rigorous approaches with more realistic assumptions (e.g., Refs. 3–14) that take into account surface heat transfer, an extended or diffuse Gaussian heat source, dependence of thermal properties on temperature, etc. All these modifications are rather complicated. One of the findings from these investigations (e.g., Ref. 8) was that the cooling rate (or cooling time) in the HAZ did not depend on the location of the point heat source and, therefore, could be found from Rosenthal's solution.

Ashby and Easterling (Ref. 4) simplified the two limiting solutions derived by Rosenthal to obtain temperature/time profiles in the HAZ. One set of solutions was derived for thick plates (assuming 3-D heat flow) and the other for thin plates (assuming 2-D heat flow). There is also an equation to determine a critical thickness for a given heat input (or a critical heat input for a given plate thickness, if used in reverse) at which the 2-D condition changes to 3-D (Ref. 15). There have also been some attempts to define dimensionless parameters that define the transition point between 2-D and 3-D conditions (Refs. 16, 17). However, these criteria may be too simplistic. Real welds are more likely to lie between the two limiting solutions: a situation classified by some researchers as 2.5-D (Ref. 16),for which there is no simple solution (Ref. 1). The question then is where a particular case lies with respect to the 2-D and 3-D conditions. The objective of this paper is to introduce a simple method to answer the above question. The goal is to find the actual values of parameters (as opposed to the lower-bound or upper-bound values), such as cooling rate and peak temperature profile, for a given weld section. This can be very useful as experimental measurement of weld thermal cycles, e.g., by embedding thermocouples in the HAZ, is in some cases impractical considering the small size of the HAZ. The approach, explained in the next section, is based on deriving a parameter (i.e., HAZ width) that can be measured by sectioning a sample, and using this parameter to calculate a

KEYWORDS

Cooling Rate
Heat-Affected Zone
Weld Thermal Cycle
Instrumented Welding
Transformable Steels
Rosenthal's Analytical Solutions
Gas Tungsten Arc Welding
Heat Input

K. POORHAYDARI (kioumars@ualberta.ca), *D. G. IVEY, and B. M. PATCHETT are with the Department of Chemical and Materials Engineering, University of Alberta, Alberta, Canada.*

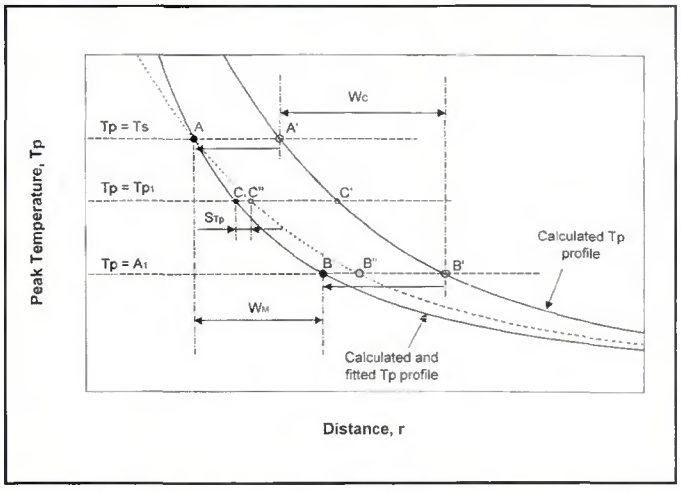

Fig. 1 — Schematic for calibration (shifting and fitting) of the calculated peak temperature profile.

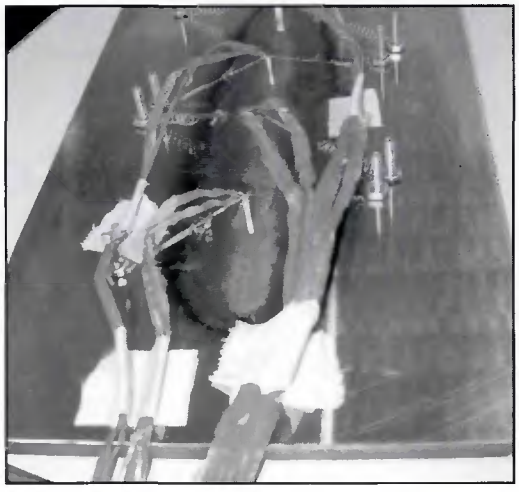

Fig. 2 — Thermocouple/plate attachment on the bottom of the plate. The image was taken after welding.

Table 1 — Definition, Units, and Values (for Carbon Steel) of the Parameters Used in Equations 1–9 (Ref. 4)

Symbol	Definition and unit	Value
T	Temperature, °C (°F)	—
T_P	Peak temperature, °C (°F)	—
t	Time, s	—
Δt_{8-5}	Cooling time from 800° to 500°C, s	—
r	Radial/lateral distance from weld, m (in.)	—
T_0	Initial temperature, °C (°F)	25 (77)
λ	Thermal conductivity, $Js^{-1}m^{-1}°C^{-1}$ ($Js^{-1}in.^{-1}°F^{-1}$)	41 (1.87)
a	Thermal diffusivity, m^2/s ($in.^2/s$)	9.1×10^{-6} (14.1 x 10^{-3})
ρc	Specific heat per unit volume, $Jm^{-3}°C^{-1}$ ($Jin.^{-3}°F^{-1}$)	4.5×10^6 (0.13 x 10^3)
d	Plate thickness, m (in.)	8×10^{-3} (0.31)
q	Arc power, J/s	—
v	Travel speed, m/s (in./s)	—
q/v	Heat input, J/m (J/in.)	—

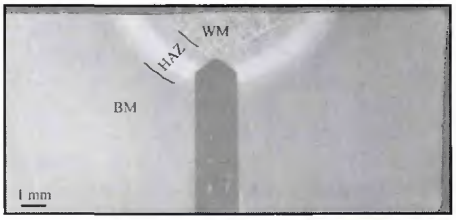

Fig. 3 — Transverse section of a 0.5 kJ/mm (12.7 kJ/in.) weld sample showing the location of a thermocouple tip in the HAZ. The dark background area is Bakelite™ used for metallographic mounting. The other regions are base metal (BM) and weld metal (WM).

weighting factor to apply to the thick- and thin-plate values of the parameters of interest. To compare the calculations with experimental data, limited instrumented autogenous GTAW (gas tungsten arc welding with thermocouples embedded in horizontal flat plates) was performed to record the thermal cycles with a data a quisition system.

Theoretical Approach

The two limiting solutions to the Rosenthal equations of a moving point heat source for regions outside the fusion zone are laid out below (Ref. 15). The solutions give the temperature variation during cooling as a function of time for a given location, the peak temperature (T_P) as a function of distance from the heat source, and the weld time constant (Δt_{8-5}), which is the cooling time from 800° to 500°C (1472° to 932°F).

Thick plates (3-D):

$$T - T_0 = \frac{q/v}{2\pi\lambda t} exp\left(-\frac{r^2}{4at}\right) \quad (1)$$

$$T_P - T_0 = \left(\frac{2}{\pi e}\right)\frac{q/v}{\rho c r^2} \quad (2)$$

$$\Delta t_{8-5} = \frac{q/v}{2\pi\lambda\theta_1} \quad (3)$$

$$\frac{1}{\theta_1} = \left(\frac{1}{500 - T_0} - \frac{1}{800 - T_0}\right) \quad (4)$$

Thin plates (2-D):

$$T - T_0 = \frac{q/v}{d\left(4\pi\lambda\rho ct\right)^{1/2}} exp\left(-\frac{r^2}{4at}\right) \quad (5)$$

$$T_P - T_0 = \left(\frac{2}{\pi e}\right)^{1/2} \frac{q/v}{d\rho c 2r} \quad (6)$$

$$\Delta t_{8-5} = \frac{\left(q/v\right)^2}{4\pi\lambda\rho c d^2\theta_2} \quad (7)$$

$$\frac{1}{\theta_2} = \left(\frac{1}{\left(500 - T_0\right)^2} - \frac{1}{\left(800 - T_0\right)^2}\right) \quad (8)$$

$$d_C = \left[\frac{q/v}{2\rho c}\cdot\left(\frac{1}{500 - T_0} + \frac{1}{800 - T_0}\right)\right]^{1/2} \quad (9)$$

The parameters in the above equations are defined and their values are reported in Table 1. Equation 9 calculates the critical plate thickness, d_C, over which the crossover between the 2-D and 3-D conditions of heat flow takes place (Ref. 15). Note that the unique characteristic of

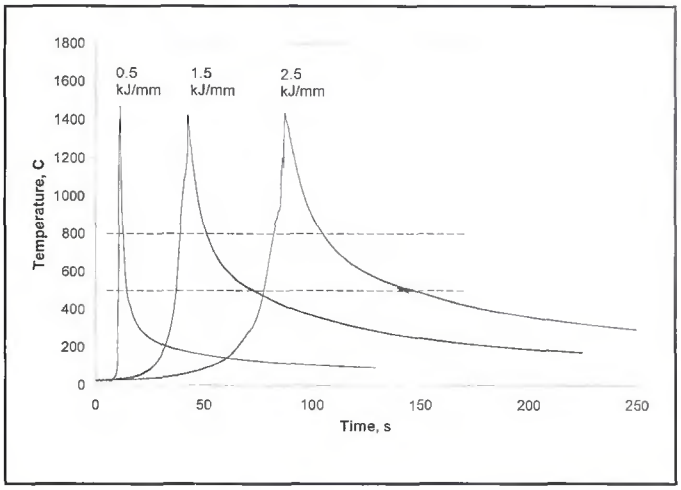

Fig. 4 — The actual weld thermal cycles measured in the HAZ close to the weld interface for different weld samples with heat inputs of 0.5, 1.5, and 2.5 kJ/mm (12.7, 38.1, and 63.5 kJ/in.). The cooling time from 800° to 500°C (1472° to 932°F) increases dramatically as the heat input increases.

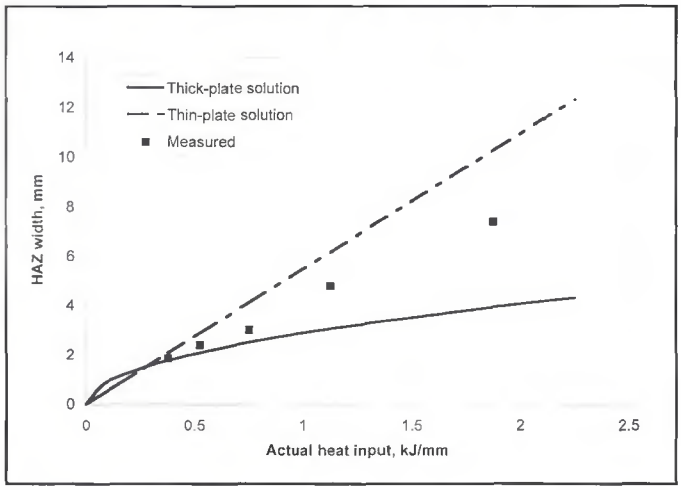

Fig. 5 — Variation of HAZ width with heat input. The experimental values lie between the upper- and lower-bound lines (thin- and thick-plate solutions) predicted from the Rosenthal theory.

cooling rate is that it is independent of the distance from the heat source, at least in the HAZ. This fact has also been confirmed by numerical analysis (e.g., Ref. 18) as well as experiments (e.g., Ref. 19), where researchers have found that cooling rate is only dependent on heat input, plate geometry/thickness, and plate initial temperature (i.e., preheating). This assumption is widely accepted in the welding industry (e.g., Refs. 12, 15, 20). One abstract parameter appearing in these equations is heat input, q/v, which in electric arc processes is defined as

$$q/v = \frac{E.I.\eta}{v} \tag{10}$$

E is the arc voltage in V, I is arc current in A, and η is the thermal efficiency. Thermal efficiency, which is in fact the ratio between the actual heat input to the workpiece and the energy output of the welding machine, is lower than 1, because some part of the arc energy is dissipated to the surroundings by radiation, convection, or conduction, and is therefore lost. In this paper, the term actual heat input (a.k.a. *effective* heat input or *net* heat input) refers to q/v with $\eta < 1$, and the term nominal heat input refers to q/v with $\eta = 1$.

The main idea here is to evaluate the actual state of heat flow, whether 2-D, 3-D, or something in between, for which the actual response of the joint to the weld thermal cycle can be used. It is well known that the visible HAZ boundaries in transformable steels correspond to the T_S (solidus temperature or peritectic temperature) on the side adjacent to the weld zone and to the Ac_1 (the lower critical temperature upon heating), or simply A_1 (Ref. 15), on the side adjacent to the unaffected base metal. Therefore, the HAZ width, W, can be simply formulated as

$$W = r_{A1} - r_{Ts} \tag{11}$$

Finding r_{A1} and r_{Ts} from Equations 2 and 6 and substituting them into Equation 11 will yield the HAZ width for thick- and thin-plate assumptions, respectively:

$$W_{Thick-plate} = C_1 \cdot \left(q/v\right)^{\frac{1}{2}} \tag{12}$$

$$C_1 = \left[\frac{2}{\pi e \rho c}\right]^{\frac{1}{2}} \cdot \left[\frac{1}{\left(A_1 - T_0\right)^{\frac{1}{2}}} - \frac{1}{\left(T_S - T_0\right)^{\frac{1}{2}}}\right] \tag{13}$$

$$W_{Thin-plate} = C_2 \cdot (q/v) \tag{14}$$

Table 2 — HAZ Widths and Weighting Factors for Three Weld Samples

Nominal heat input, kJ/mm (kJ/in.)	HAZ width, mm (in.) Thick-plate (Eq. 12)	Thin-plate (Eq. 14)	Measured	Weighting factor, F (Eq. 19)
0.5	1.76	2.05	1.86	0.34
(12.7)	(0.069)	(0.081)	(0.073)	
1.5	3.05	6.16	4.80	0.56
(38.1)	(0.120)	(0.243)	(0.189)	
2.5	3.93	10.27	7.40[a]	0.55
(63.5)	(0.155)	(0.404)	(0.291)	

(a) An estimated value based on the extension of the HAZ boundary curves, as the HAZ/BM boundary intersects the bottom of the plate for the heat input of 2.5 kJ/mm.

$$C_2 = \left[\frac{2}{\pi e}\right]^{\frac{1}{2}} \cdot \left[\frac{\left(T_S - A_1\right)}{2d\rho c\left(T_S - T_0\right)\left(A_1 - T_0\right)}\right] \tag{15}$$

Based on the assumption that the actual situation lies between the two limiting solutions, the actual HAZ width can be related to the above values (Equations 12 and 14) as

$$W_{Actual} = W_{Thick-plate} + F \cdot (W_{Thin-plate} - W_{Thick-plate}) \tag{16}$$

F, varying between 0 and 1, is the weighting factor that calculates the deviation from the thick-plate solution with respect to the thin-plate solution. It can be shown that Equation 16 can be easily derived, if the same kind of relationship for estimation of r_{A1} and r_{Ts} was considered initially (i.e., the following equations), and

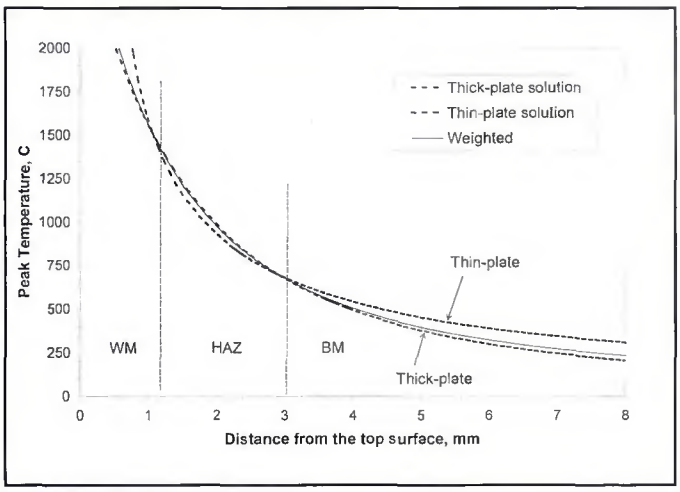

Fig. 6 — Calibrated peak temperature profiles for a nominal heat input of 0.5 kJ/mm (12.7 kJ/in.). The weighted profile is plotted along with the thick- and thin-plate solutions.

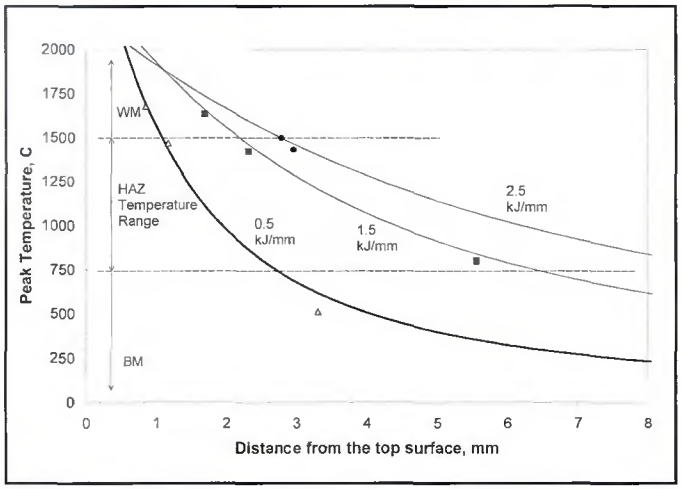

Fig. 7 — Peak temperature profiles weighted and fitted for three different weld samples; heat input values of 0.5, 1.5, and 2.5 kJ/mm (12.7, 38.1, and 63.5 kJ/in.).

Table 3 — Cooling Time and Cooling Rate from 800° to 500°C (1472° to 932°F) for Three Weld Samples

Nominal heat input, (kJ/mm) (kJ/in.)	Cooling time (Δt_{8-5}), s				Mean cooling rate, °C/s (°F/s) (Eq. 26)	
	Thick-plate (Eq. 3)	Thin-plate (Eq. 7)	Estimated (Eq. 20)	Measured	Estimated	Measured
0.5 (12.7)	1.2	2.6	1.7	1.8±0.1	178.8 (321.8)	171.0±6.2 (307.8±11.2)
1.5 (38.1)	3.6	23.6	14.8	17.2±1.5	20.2 (36.4)	16.8±1.2 (30.2±2.2)
2.5 (63.5)	5.9	65.6	38.6	37.7±10.1	7.8 (14.0)	8.0±2.9 (14.4±5.2)

then substituted into Equation 11.

$$r_{A1\text{-}Actual} = r_{A1\text{-}Thick\text{-}plate} + F \cdot (r_{A1\text{-}Thin\text{-}plate} - r_{A1\text{-}Thick\text{-}plate}) \quad (17)$$

$$r_{Ts\text{-}Actual} = r_{Ts\text{-}Thick\text{-}plate} + F \cdot (r_{Ts\text{-}Thin\text{-}plate} - r_{Ts\text{-}Thick\text{-}plate}) \quad (18)$$

Rearranging Equation 16 gives the value of F for any given weld sample:

$$F = (W_{Actual} - W_{Thick\text{-}plate}) / (W_{Thin\text{-}plate} - W_{Thick\text{-}plate}) \quad (19)$$

It is proposed that the thermal parameters of importance can be estimated by weighting the thick- and thin-plate solutions, using the weighting factor F:

$$\Delta t_{Actual} = \Delta t_{Thick\text{-}plate} + F \cdot (\Delta t_{Thin\text{-}plate} - \Delta t_{Thick\text{-}plate}) \quad (20)$$

$$T_{P,Actual} = T_{P,Thick\text{-}plate} + F \cdot (T_{P,Thin\text{-}plate} - T_{P,Thick\text{-}plate}) \quad (21)$$

Equation 20 is similar to one proposed by Hess et al. (Ref. 19), who proposed that a "correction factor," which would represent "the degree of infiniteness," should be calculated by measuring the instantaneous cooling rate at a particular time from an experimentally obtained thermal cycle. This value would then be compared with the corresponding values obtained from Rosenthal's equations for thick- and thin-plate conditions through Equation 20. This correction factor would be used to obtain corrected values of cooling rate at other times (or temperatures). The approach adopted here, and shown to be reliable in the next section, demonstrates that the correction factor can be obtained from the measurement of the HAZ width independently, and therefore the instrumented welding test can be eliminated.

Note, as mentioned earlier, the location of the heat source does not affect the cooling rate but shifts the peak temperature profile relative to the plate geometry. In reality, the heat source may not coincide with the top surface of the plate. Going back to the fundamental assumption that the location and peak temperatures of the HAZ boundaries are known, the exact peak temperature profile can be plotted with respect to the distance from the top surface of the plate, which is a tangible reference point. Figure 1 shows schematically how a calculated profile (either based on thick-plate/thin-plate assumptions or weighted as proposed by Equation 21) is shifted and fitted into the known locations designated by points A (representing the solidus temperature) and B (representing the A_1 temperature). Equation 22 formulates this mathematically.

$$r^*_{Tp} = r_{Tp} - \left(r_{Ts} - r^*_{Ts}\right) - S_{Tp} \quad (22)$$

$$S_{Tp} = (W_C - W_M) \cdot \frac{T_S - T_P}{T_S - A_1} \quad (23)$$

The symbol * on r values in Equation 22 designates the distance of a given point in the plate (specified by a peak temperature) from the top surface. Otherwise, r designates the distance with reference to the heat source. Therefore, r_{Tp} values are a series of points for which T_P is calculated from Equation 21; r_{Ts} is one of these points where $T_P = T_S$, and r^*_{Ts} is measured from the weld section. W_C and W_M are the calculated and measured values, respectively, of the HAZ width. As shifting the entire curve from the point A' to A in Fig. 1 (represented by the initial terms in Equation 22) may move an arbitrary point C' to C" and not necessarily to C, a further adjustment is needed. This adjustment is represented by the term S_{Tp} in Equation 22 and calculated from Equation 23, which provides an additional shift (e.g.,

point C" to C or point B" to B) proportional to the temperature difference in T_P from the reference point used here (i.e., T_S). Note that this adjustment is also proportional to the difference between the calculated and measured values of the HAZ width, which is considerable when the calculations are based on thick- or thin-plate assumptions. For the case where calculation of peak temperature is based on weighted values (i.e., Equation 21), the adjustment is minimal (even null theoretically as the calculated width should represent the actual width in the first place, but minimal due to accumulated errors from rounding throughout the calculations).

The following equations can be used to find the critical temperatures A_1 and T_m (melting point, which is an upper-bound value for T_s), in case this information is not readily available. The alloying additions are in wt-% and the temperatures are calculated in K (Ref. 21).

$$A_1 = 996 - 30\,Ni - 25\,Mn - 5\,Co + 25\,Si + 30\,Al + 25\,Mo + 50\,V \quad (24)$$

$$T_m = 1810 - 90\,C \quad (25)$$

Experimental Procedure

A plate of Grade 690 microalloyed steel (containing 0.08% C and microalloyed mainly with Ti, Nb, and V), 8 mm (0.31 in.) in thickness, was used in this study. The designation 690 refers to the specified minimum yield strength in megapascal (Canadian Standards Association designation (Ref. 22)), equivalent to 100 in ksi. The plate was cut into pieces with approximate dimensions of 285 mm (11.22 in.) by 165 mm (6.50 in.) to be used for instrumented welding. The oxide scales were removed from both surfaces by milling to allow for good arc conductivity and stability, as well as to remove small bumps on the surface and make them very flat. Holes were drilled about 2 in. (50.8 mm) apart on the bottom side of the plates along the central line with variable depths. Four thermocouples (three of type K and one of type S) were used for each experiment. The type S thermocouple was used for the hole close to the weld interface, which experienced the highest temperatures. Thermocouple wires, 0.25 mm (0.010 in.) in diameter were passed through a ceramic insulator, 3.18 or 1.59 (⅛ or 1/16 in.) OD, and spot welded at one end to make the junction. The thermocouples were secured to the plate with springs as shown in Fig. 2, which provided gentle pressure on the back of the ceramic insulator to maintain contact between the thermocouple junction and the plate throughout welding.

Welding was performed using DCEN autogenous GTAW with DC current and a tungsten electrode used in negative polarity. Nominal heat inputs of 0.5, 1.5, and 2.5 kJ/mm (12.7, 38.1, and 63.5 kJ/in.) were applied by selecting an arc voltage of 12.2 V, an arc current of 150 A, and travel speeds of ~ 3.6, 1.2, and 0.7 mm/s, respectively. After welding, the plates were precision cut transversely from the center of the thermocouple holes, and then mounted, ground, polished, and etched, to reveal the weld interface and the HAZ. Figure 3 shows a cross section for one of the samples.

Results and Discussion

Figure 4 shows representative thermal cycles (for three different heat inputs), experimentally obtained at locations close to the weld interface. The thermal cycle is very fast for a nominal heat input of 0.5 kJ/mm (12.7 kJ/in.) and gets considerably slower as the heat input increases to nominal values of 1.5 and 2.5 kJ/mm (38.1 to 63.5 kJ/in.). The curves (not all shown here) were analyzed to obtain cooling times and peak temperature profiles, as described below.

Weighting Factors

Figure 5 compares the values of the HAZ width measured directly below the centerline (on sections without the thermocouple holes) for several weld samples (nominal heat inputs 0.5–2.5 kJ/mm), with the theoretical thick- and thin-plate solutions found from Equations 12 to 15. Additional weld samples with nominal heat inputs of 0.7 and 1.0 kJ/mm, produced without thermocouple instrumentation, were sectioned and their HAZ widths are included in Fig. 5. Again the welding parameter that varied to produce the required heat input was the travel speed; other parameters were as stated earlier. These additional samples provided data to see if the HAZ width was linear with respect to the heat input. As shown in Fig. 5, the dependence deviates from linearity. The calculated weighting factors for the three weld samples, for which instrumented welding was performed, are reported in Table 2.

A value of Ae_1 = 695°C (1283°F) was used here, which was obtained from the CCT (continuous cooling transformation) diagram for the specific Grade 690 microalloyed steel (Ref. 23). This value is somewhat higher than the equilibrium value of A_1 = 684°C (1263°F) obtained from Equation 24. As Equation 25 calculates T_m rather than the solidus temperature, a value of T_S = 1500°C (2732°F) was used here, which is slightly lower than the T_m = 1530°C (2786°F) obtained from Equation 25. This value also lies between the peritectic temperatures for the Fe-C and Fe-Mn binary systems (i.e., 1493° and 1504°C, or 2719° and 2739°F, respectively (Ref. 24)). A value of η = 0.75 was used in Equation 10 to obtain the actual values of heat input. Thermal efficiency is not easy to determine, as it depends on many factors such as the weld process, welding equipment and setup, travel speed, the material to be welded (anode work function), arc voltage, and current. In GTAW, thermal efficiency is highest for DCEN and increases as the travel speed increases. Fuerschbach and Knorovsky (Ref. 25) reported arc efficiencies of around 0.7–0.8 for GTAW-DCEN after conducting calorimetric tests on several steels and a Ni-based alloy. Arc efficiency reached a plateau of 0.8 as the travel speed increased. Values within the same range were also confirmed by Kou (Ref. 26) and used by others (e.g., Ref. 12). Although much lower values for the thermal efficiency in GTAW have been reported in the literature elsewhere (e.g., Refs. 1, 5, 15), a value of η = 0.75 obtained through more recent calorimetric experiments was deemed to be more reasonable for the setup and welding characteristics used here, which is in agreement with the value reported in the *ASM Handbook* (Ref. 27).

The finding that the experimental values for lower heat-input samples are closer to the thick-plate solution in Fig. 5 is reasonable, as the weld zone sizes for these samples are relatively small with respect to the thickness of the plate. Using Equation 9 in reverse gives a critical heat input of 0.17 kJ/mm (4.3 kJ/in.), corresponding to a nominal heat input of 0.23 kJ/mm (5.7kJ/in.) assuming η = 0.75, for a fixed plate thickness of 8 mm (0.31 in.). However, as can be seen, assuming heat transfer behavior is 2-D above the critical value is not reasonable, as none of the actual data lie on the thin-plate solution line. For the 2-D situation to prevail, the weld metal zone should span over the whole width of a thin plate, so that the heat transfer occurs only within the plane of the plate, which is not the case even for the highest heat input used here.

Cooling Time/Rate

Table 3 compares the predicted values of cooling time and cooling rate for nominal heat inputs of 0.5, 1.5, and 2.5 kJ/mm (12.7, 38.1, and 63.5 kJ/in.), with those experimentally obtained. Note, that mean cooling rate for the temperature range 800° to 500°C (1472° to 932°F) is calculated in °C/s from a simple equation:

$$T'_{800-500} = \frac{300}{\Delta t_{8-5}}. \quad (26)$$

The experimental values reported in Table 3 are the arithmetic means among the thermocouple readings, as long as the peak temperature is above 800°C (1472°F). The predicted range of cooling times for a 0.5 kJ/mm (12.7 kJ/in.) weld sample was found to be between 1.2 and 2.6 s. This translates to mean cooling rates approximately between 110° and 250°C/s (~200° to 450°F/s). The predicted ranges of mean cooling rates for the other weld samples were found to be approximately 13°–85°C/s (23°–153°F/s) for a heat input of 1.5 kJ/mm (38.1 kJ/in.) and 5°–50°C/s (9°–90 °F/s) for a heat input of 2.5 kJ/mm (63.5 kJ/in.). The wide range of cooling values suggests a great deal of uncertainty. Having more specific numbers, using the method proposed here, is essential for any simulation or microstructure/property correlation studies.

The standard deviation of measured cooling time values increased relative to the average value as the heat input increased due to heat accumulation in the plate during welding. Heat accumulation increased the effective initial temperature in the plate as welding continued. For instance, the first thermocouple for 2.5 kJ/mm (63.5 kJ/in.) welding recorded a cooling time of 23.5 s while the next three thermocouples recorded cooling times of 38.0, 42.6, and 46.8 s in sequence. This phenomenon would not happen for lower heat inputs (low relative to the thickness and area of the plate), as the travel speed would be high enough to minimize the temperature rise during welding. Using a larger plate would also result in a smaller standard deviation. Nevertheless, the range is still much smaller than the range between the thick- and thin-plate values.

Peak Temperature Profiles

A weighted peak temperature profile, obtained from Equation 21 and calibrated by Equation 22, is shown in Fig. 6 (solid line) for a weld sample with a nominal heat input of 0.5 kJ/mm (12.7 kJ/in.). The theoretical results with thin- and thick-plate assumptions are also plotted (dashed lines). All profiles are calibrated with respect to the actual plate geometry and location of the HAZ boundaries according to Equation 22, to show the differences in the shapes (curvatures) only. As can be seen, the different assumptions do not markedly change the shape of the peak temperature profiles. For this heat input (0.5 kJ/mm), the corresponding weighting factor (Table 2) predicts a profile with a shape close to that predicted by the thick-plate solution.

The weighted and calibrated peak temperature profiles for the three values of heat input were determined and are plotted in Fig. 7. Some of the values experimentally obtained are indicated too. Contact between the thermocouple tip and the plate was not well maintained for all thermocouples throughout welding. Therefore, only those that maintained good contact are reported here. Spot welding of the thermocouple junctions to the plate (e.g., Ion et al. (Ref. 21)) would be ideal, as the best response time is expected from small bead volumes with maximized surface contact. Spot welding at the bottom of drilled holes was impractical for the present setup, consisting of small-diameter holes and small thermocouple junction sizes.

Applications and Limitations

The thermal cycles and the calculated peak temperature profiles have been used for kinetic analysis of carbide particle dissolution and coarsening in the HAZ, while the cooling rate estimations have been used for interpretation of phase transformations and carbide reprecipitation (Ref. 28). Although this approach was geared to transformable steels in this paper, it is expected that the concept can be applied to other materials, as long as the HAZ has visible boundaries in the etched macro section and the peak temperatures for the boundaries are known.

One important practical point in examining the weld weld zone, or in selecting the welding parameters to reach a certain cooling rate in the joint, is that cooling rate is not the same in all radial directions on a transverse section. It has been observed experimentally in very early measurements (Ref. 19) that on plates of intermediate thickness (2.5-D heat flow condition), the cooling rate is higher at the top of the plate adjacent to either side of the bead than at the bottom (directly under the deposited metal) and the HAZ width is smaller. This is due to the difference in the availability of quenching material at different radial directions. It is expected that the method of correction, based on HAZ width presented here, will be capable of determining the actual cooling rate along the direction of interest, by measuring the HAZ width along that direction. This requires more investigation. Note that some uncertainty about the material thermal properties and/or welding parameters may be less important for the proposed method. The proposed method compares theoretical solutions with, and fits them to, the actual behavior of the welded section, whose behavior is based on effective values of the thermal parameters, probably unknown to the investigator.

The method introduced in this paper was used for bead-on-plate or autogenous welding on flat plates, which is used widely for mechanical and microstructural examinations of the weld HAZ. One should note that the original Rosenthal thick- and thin-plate solutions were derived for such conditions. The general concept behind the method, however, may be applied to weld sections with other geometries, as long as the initial upper-bound and lower-bound equations applicable to those geometries are available, or the Rosenthal solutions are modified so that they can be applied to other geometries. This also needs further investigation. Examination of a wider range of welding variables needs to be considered as future work.

Summary

An innovative method for estimation of cooling rate in a welded section was presented in this paper. The method is based on applying a weighting factor to the Rosenthal analytical solutions for thick and thin plates. The factor is determined from the HAZ width, obtained from etched sections, which reflects the actual response of the plate to the heat flow conditions. While the lower- and upper-bound solutions to Rosenthal's equation, derived by assuming thick- and thin-plate conditions, provide a wide range of values for cooling rate during the weld thermal cycle, the method and formulations presented here yielded specific numbers very close to those obtained experimentally. The advantage of this method is the simplicity of the calculations and the experimental procedure; only a macro-etched weld section is needed. Instrumented welding tests (by embedding thermocouples) can be eliminated. The method was also used to obtain a weighted peak temperature profile and to calibrate the shape and size of the profile.

The method was applied only to horizontal flat plates, where the Rosenthal equations directly apply. More work is needed for application of this method (or the general idea) to plates with other geometries/positions and examination of a wider range of welding variables. Nevertheless, the limited experimental work has demonstrated the promise of this simple method, as a first step in the extraction of useful information from a weld HAZ section that contains thermal history information. This information can be applied to correlation studies involving microstructure, simulation, and modeling.

Acknowledgments

The authors wish to thank the National Sciences and Engineering Research Council (NSERC) of Canada and IPSCO

Inc. for their financial support of this project. The authors are also grateful to Clark Bicknell for welding, Les Dean for writing the LabVIEW 5.0 code for thermal data acquisition, and Walter Boddez for discussions on thermocouple fabrication and supply purchases.

References

1. Rosenthal, D. 1941. Mathematical theory of heat distribution during welding and cutting. *Welding Journal* 20(5): 220-s to 234-s.

2. Rosenthal, D. 1946. The theory of moving sources of heat and its application to metal treatments. *Trans. ASME* 48: 848–866.

3. Adams, C. M., Jr. 1958. Cooling rates and peak temperatures in fusion welding. *Welding Journal* 37(5): 210-s to 215-s.

4. Ashby, M. F., and Easterling, K. E. 1982. A first report on diagrams for grain growth in welds. *Acta Metall.* 30(11): 1969–1978.

5. Christensen, B. N., Davies, V. D. L., and Gjermundsen, K. 1965. Distribution of temperatures in arc welding. *British Welding Journal* (February): 54–75.

6. Eagar, T. W., and Tsai, N.-S. 1983. Temperature fields produced by traveling distributed heat sources. *Welding Journal* 62(12): 346-s to 355-s.

7. Grosh, R. J., and Trabanat, E. A. 1956. Arc-welding temperatures. *Welding Journal* 35(8): 396-s to 400-s.

8. Kasuya, T., and Yurioka, N. 1993. Prediction of welding thermal history by a comprehensive solution. *Welding Journal* 72(3): 107-s to 115-s.

9. Nunes, A. C., Jr. 1983. An extended Rosenthal weld model. *Welding Journal* 62(6): 165-s to 170-s.

10. Rykalin, N. N., and Bekerov, A. I. 1967. Calculating the thermal cycle in the heat-affected zone from the two-dimensional outline of the molten pool. *Welding Production* 14(9): 42–47.

11. Tanaka, S. 1943. A study on heat conduction of a moving heat source. *Journal Japan Welding Society* 13(9): 347–359.

12. Shah, A. K., Kulkarni, S. D., Gopinathan, V., and Krishnan, R. 1995. Weld heat-affected zone in Ti-6Al-4V alloy, Part 1: Computer simulation of the effect of weld variables on the thermal cycles in the HAZ. *Welding Journal* 74(9): 297-s to 304-s.

13. Kou, S. 1981. Simulation of heat flow during the welding of thin plates. *Metall. Transactions A.* 12A(12): 2025–2030.

14. Goldak, J., Chakravarti, A., and Bibby, M. 1984. A new finite element model for welding heat sources. *Metall. Trans. B.* 15B(2): 299–305.

15. Easterling, K. E. 1992. *Introduction to the Physical Metallurgy of Welding*. 2nd ed, Oxford, U.K.: Butterworth-Heinemann Ltd.

16. Myers, P. S., Uyehara, O. A., and Borman, G. L. 1967. Fundamentals of heat flow in welding. *Weld. Res. Council Bull.* 123: 1–46.

17. Tsai, C. L., and Tso, C. M. 1993. Heat flow in fusion welding. *ASM Handbook*, Vol. 6: *Welding, Brazing and Soldering.* Materials Park, Ohio: ASM International, pp. 7–18.

18. Zhang, W., Elmer, J. W., and DebRoy, T. 2002. Modeling and real time mapping of phases during GTA welding of 1005 steel. *Materials Science and Engineering A* (Switzerland) 333 (1-2): 320–335.

19. Hess, W. F., Merill, L. L., Nippes, E.F., Jr., and Bunk, A. P. 1943. The measurement of cooling rates associated with arc welding and their application to the selection of optimum welding conditions. *Welding Journal* 22(9): 377-s to 422-s.

20. Collins, L. E., Godden, M. J., and Boyd, J. D. 1983. Microstructures of linepipe steels. *Can. Metall. Q.* 22(2): 169–179.

21. Ion, J. C., Easterling, K. E., and Ashby, M. F. 1984. A second report on diagrams of microstructure and hardness for heat-affected zones in welds. *Acta Metall.* 32(11): 1949–1962.

22. CSA Standard Z245.1-02, *Steel Pipe*. 2002. Canadian Standards Association.

23. CCT diagram for Grade 690 microalloyed steel. Private communication between D. G. Ivey and L. Collins, IPSCO, Inc.

24. Hansen, M. 1958. *Constitution of Binary Alloys*. Second ed., New York, N.Y.: McGraw-Hill.

25. Fuerschbach, P. W., and Knorovsky, G. A. 1991. A study of melting efficiency in plasma arc and gas tungsten arc welding. *Welding Journal* 70(11): 287-s to 297-s.

26. Kou, S. 2003. Heat flow in welding. *Welding Metallurgy*, 37–43, Hoboken, N.J., Wiley-Interscience.

27. Key, J. F. 1993. Arc physics of gas-tungsten arc welding. *ASM Handbook*, Vol. 6: *Welding, Brazing, and Soldering*. Materials Park, Ohio: ASM International, pp. 30–35.

28. Poorhaydari, K. 2005. Microstructure and property examination of weld HAZ in Grade 100 microalloyed steel. PhD dissertation. Edmonton, University of Alberta.

CAN WE TALK?

The *Welding Journal* staff encourages an exchange of ideas with you, our readers. If you'd like to ask a question, share an idea or voice an opinion, you can call, write, e-mail or fax. Staff e-mail addresses are listed below, along with a guide to help you interact with the right person.

Publisher/Editor
Andrew Cullison
cullison@aws.org, Extension 249
Article Submissions

Senior Editor
Mary Ruth Johnsen
mjohnsen@aws.org, Extension 238
Feature Articles

Associate Editor
Howard Woodward
woodward@aws.org, Extension 244
Society News
Personnel

Assistant Editor
Kristin Campbell
kcampbell@aws.org, Extension 257
New Products
News of the Industry

Managing Editor
Zaida Chavez
zaida@aws.org, Extension 265
Design and Production

Advertising Sales Director
Rob Saltzstein
salty@aws.org, Extension 243
Advertising Sales

Advertising Production Coordinator
Frank Wilson
fwilson@aws.org, Extension 465
Advertising Production

Advertising Sales & Promotion Coordinator
Lea Garrigan
garrigan@aws.org, Extension 220
Production and Promotion

Peer Review Coordinator
Doreen Kubish
doreen@aws.org, Extension 275
Peer Review of Research Papers

Welding Journal Dept.
550 N.W. LeJeune Rd.
Miami, FL 33126
(800) 443-9353
FAX (305) 443-7404